AIAA 98-0159

Characterization of Laser-Heated Soot Particles Using Optical Pyrometry

K.R. McManus, J.H. Frank, M.G. Allen, and W.T. Rawlins
Physical Sciences Inc.
20 New England Business Center
Andover, MA 01810

36th Aerospace Sciences Meeting & Exhibit

January 12-15, 1998 / Reno, NV

CHARACTERIZATION OF LASER-HEATED SOOT PARTICLES USING OPTICAL PYROMETRY

K.R. McManus[*], J.H. Frank[†], M.G. Allen[‡], and W.T. Rawlins[*]
Physical Sciences Inc.
20 New England Business Center
Andover, MA 01810

Abstract

An optical probe for the measurement of soot emissions from gas turbine combustors is under development. The probe is based on laser-induced incandescence (LII) which concerns the rapid heating of soot particles using a pulsed laser and detection of the intense thermal emission from the particles. We give a brief description of a heat transfer model used to describe the transient thermal characteristics during the LII process. Experimental results obtained in simple laboratory flames are presented. An investigation of the LII signature on a timescale of the same order as the laser pulse duration (10.8 ns) suggests that incident laser intensities in excess of 12 MW/cm^2 can perturb the particle properties and likely will result in particle mass loss. This result is consistent with previously reported results.[1] A gated monochromator was used to measure particle cooling characteristics after the laser pulse. The measured cooling rates are in good agreement with model predictions in the conductive cooling regime. The results suggest that LII may be used as a diagnostic for both soot volume fraction and particle size distributions in combustion flows.

Introduction

Soot particles exhausted by jet engines on takeoff and in cruise are important contributions to atmospheric pollution, are subject to ever stricter environmental regulations, and give rise to detectable plume emissions. Current soot measurement practices used in jet engine test stands require probe sampling and off-line specimen analysis. Soot measurements performed in this manner have proven tedious and suffer from poor

_____
*Principal Research Scientist, Member AIAA
†Principal Scientist
‡Manager, Aeropropulsion Technology, Member AIAA

sensitivity. Gas turbines currently under development produce significantly lower soot emissions than those in the past, and the probe sampling techniques are proving to be greatly inadequate. Continuing efforts to characterize and control aircraft emissions of soot would benefit greatly from a commercial-scale diagnostic for gas turbine exhausts.

Physical Sciences Inc. (PSI) has performed fundamental research in evaluating the LII technique for quantitative determinations of soot volume fraction and mean particle size in sooting laminar flames. We have used a combination of LII and line-of-sight laser extinction to detect and quantify soot particles in and above methane-air and ethylene-air flames produced by a laboratory flat-flame burner.[1] The measurements include quantitative observations of the spectral distribution of incandescence from laser irradiated soot particles and the effect of the laser irradiation on the total extinction of a weak probe beam. In addition, we have examined the onset of vaporization of the soot particles by the pulsed laser beam and have determined the resulting mass-loss characteristics. These previous experimental results suggest that a simple diagnostic probe may be designed for soot measurements in practical combustion environments.

The present paper describes results from experiments being performed to direct probe design and development. Measurement parameters addressed in this paper include the excitation laser intensity and the detection system time response. In the following section, the theory concerning transient heat transfer of laser heated particles is briefly reviewed. Then, experimental results will be described indicating the effects of the pump laser intensity on the observed thermal emission signature. Results from temporally resolved LII measurements are then compared with the theoretical model to estimate soot primary particle size. Finally, a discussion of the observed experimental results will be presented.

Theoretical Considerations

The irradiation and heating of small soot particles by a pulsed, high-intensity laser results in an intense thermal emission signature whose intensity is proportional to the initial soot volume fraction.[2,3] From the transient emission signature it is possible to extract information concerning the particle size distribution due to the dependence of particle heat transfer on particle size. To understand the qualitative trends observed in detected LII emission signatures, it is useful to write an energy balance for a flame generated soot particle in the presence of laser heating. The time-dependent LII process can be described by a pair of coupled differential equations describing the heat balance for a given particle size and the change in particle size due to vaporization:

$$V_p \rho_s c_s \; dT/dt \; = \; Q_{absorption} \; + \; Q_{conduction} \; + \; Q_{vaporization}$$
$$+ \; Q_{radiation} \; + \; Q_{thermionic}$$
$$\rho_s \; dr/dt \; = \; -\rho_v U_v$$

where V_p is the volume of the particle, ρ_s and c_s are the density and specific heat of soot, the Q's denote heat gains or losses in W/particle, and ρ_v and U_v are the density and velocity of the vaporized carbon. Numerical integration of these equations gives a predicted temperature and spectral radiation history for each particle size, which can be combined with a particle size distribution to describe the entire LII process for a given ensemble of soot particles. However, there are several sources of uncertainty in this basic model, including the formulations of the heat loss terms, the values for some of the thermodynamic parameters for soot and its vapor, the effects of the radial intensity profile of the laser beam, and the basic physics associated with non-spherical particle shape and the thermal responses of small particles to high-intensity laser pulses. These factors require in-depth theoretical and experimental investigation, where experimental measurements are used to verify theoretical descriptions.

The heat input term is the absorption of the laser radiation by the particles:

$$Q_{absorption}(r,\lambda) \; = \; \pi r^2 Q_a(r,\lambda) \; I_o(\lambda)$$
$$= \; \left(\rho_s N_o/M\right) \; V_p(r) \; \sigma_a(r,\lambda) \; I_o(\lambda)$$

where Q_a is the Mie absorption efficiency for a given particle radius and laser wavelength, and we have made the transformation from particle cross section to volume cross section. For small particles, $\sigma_a(532 \text{ nm}) \approx 7 \times 10^{-19}$ cm^2/C-atom and is essentially independent of particle size.

The heat loss from the particles is due to a combination of thermal conduction to the surrounding gas, vaporization, radiation, and thermionic emission of electrons. At high flow rates, heat can also be transferred through convection; however, this is not relevant to the flame environment, and we will not address it here. As we will show, thermal conduction and vaporization are the dominant heat loss terms for laser-heated soot. This was also found by Melton.[2]

The thermal conduction between the soot particles and the surrounding gas in atmospheric flames is best described by spherical free-molecular heat transfer.[4] This is different from the equation used by Melton, which describes continuum and transition flow with an explicit dependence on the Knudsen number, the ratio of the molecular mean free path to the particle radius. In an atmospheric flame at 1600 to 2000 K, the mean free path is approximately 450 to 600 nm. Typical soot particle sizes in such flames are $r \leq 50$ nm, giving Knudsen numbers Kn $\geq$ 10. This range of Kn is well into the free-molecular flow regime (Kn > 1), where there is no dependence of the heat transfer rate on Kn or on the thermal conductivity of the gas. For equal gas and particle velocities, the heat transfer equation for spherical geometry is[4]

$$Q_{conduction} \; = \; -\alpha/8 \; (4\pi r^2) \; (2RT/\pi)^{1/2} \; (T \; - \; T_o)$$
$$\bullet \; \rho_{gas} R(\gamma+1)/(\gamma-1)$$

where α is a molecular accommodation coefficient for collisions of air molecules with the carbon surface (typically $\approx$0.9), T_o is the temperature of the ambient gas, R is the gas constant, and γ is the specific heat ratio for the gas, c_p/c_v (7/5 for air). For r = 30 nm, the conductive heat transfer rate ranges from $\approx$3.5 x 10^{-7} W/particle at 3000 K to $\approx$7 x 10^{-7} W/particle at 4500 K. At elevated pressures and larger particle sizes which might be encountered in gas turbine combustors and simulators, the effects of continuum and transition flow (Kn < 1) need to be considered as well.

2

The heat loss due to vaporization of the carbon is given by

$$Q_{vaporization} = dm/dt \cdot \Delta H_v/M_v$$

where dm/dt is the rate of mass loss from the particle, ΔH_v is the molar enthalpy of vaporization (sublimation) of soot carbon, and M_v is the molecular weight of the carbon vapor. The description of the mass loss rate in terms of the detailed physics of the vaporization dynamics is difficult and speculative; for present purposes, we have adopted an equilibrium description[5] analogous to that of Melton.[2] The mass loss rate is given by the net mass flow rate of vapor away from the particle surface:

$$dm/dt = -\rho_v (\bar{v}/4) (4\pi r^2) \alpha_v$$

where ρ_v is the density of the vapor above the surface, $\bar{v}$ is the average thermal velocity of the vapor molecules at the particle temperature, and α_v is a vapor-surface accommodation coefficient generally taken to be unity. The vapor density ρ_v for the equilibrium vapor pressure can be determined using the Clausius-Clapeyron equation:

$$\rho_v = (1/RT) \exp[\Delta H_v(T-T^*)/(RTT^*)]$$

where T^* is the temperature at which the equilibrium vapor pressure over carbon equals 1 atm. Using the JANAF thermochemical data base for carbon at high temperatures, we have computed the equilibrium vapor pressure and composition as functions of temperature.[6] By fitting the computed vapor pressure curve to the Clausius-Clapeyron equation, we determine $T^* = 4079$ K and $\Delta H_v = 7.50 \times 10^5$ J/mole. (Actually, these fits indicate a slight variation of ΔH_v with T, 2.4% decrease from 3000 to 6000 K, which should be included in a more rigorous treatment.) The equilibrium vapor is composed of mostly C_3, with additional amounts of C_2 and C giving an average molecular weight of ≈ 33 g/mole.

Computed vaporization rates, expressed as relative mass loss per nanosecond per particle, are illustrated in Figure 1. At temperatures of roughly 4200 to 4800 K, the computed relative mass loss rates are consistent with those observed in previous work.[1] If one computes the effective radius recession due to evaporation it is evident that, for temperatures less than 4500 K, less than 1 nm of material is vaporized during the 10 ns laser pulse, so the particle size distribution is not significantly
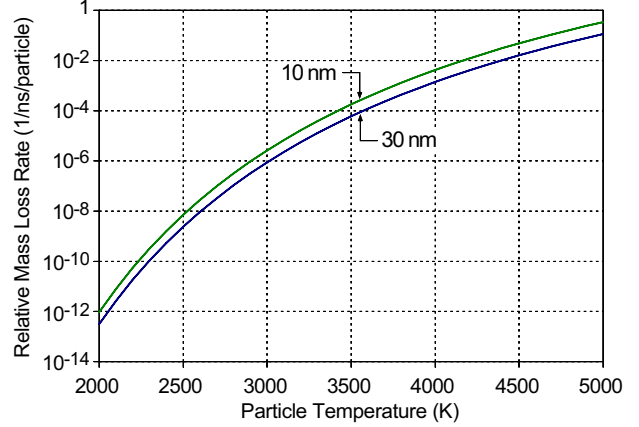
Figure 1 Vaporization relative mass loss ((dM/dt)/M, per nanosecond).

affected for pulse energies which give maximum temperatures below that level. In keeping with this, the computed heat loss due to vaporization, $Q_{vaporization}$, is steeply dependent upon particle temperature, and ranges from $\approx 5 \times 10^{-9}$ W/particle at 3000 K to $\approx 1 \times 10^{-4}$ W/ particle at 4500 K for r = 30 nm. The vaporization and conductive heat loss terms are roughly equal near 3500 K, and vaporization dominates above that temperature.

The radiative heat loss is given by

$$Q_{radiation} = -\sigma_{sb}(T^4-T_o^4) 4\pi r^2 Q_a$$

where σ_{sb} is the Stefan-Boltzmann constant, 5.6687×10^{-10} J/cm^{2}K^{4}s. For simplicity, we express Q_a as a spectrally averaged value $<Q_a>$. Mie calculations give this as ≈ 0.5 for r = 40 nm. The radiative heat loss is then calculated to be $\approx 2.5 \times 10^{-8}$ W/particle at 3000 K and $\approx 1 \times 10^{-7}$ W/particle at 4500 K, well below the conductive heat loss. Radiative heat loss does not contribute significantly to the overall energy balance, as noted by Melton.[2]

In addition to conductive, evaporative, and radiative heat loss, the particles can also lose heat through thermionic emission of electrons. This can be estimated through modification of the Richardson-Dushman equation, which describes the thermionic emission current in terms of the temperature and the work function of the material, φ_{eV}. The heat loss is

$$Q_{thermionic} = 4\pi r^2 AT^2\varphi_{eV} \exp[-\varphi_{eV}/kT]$$

where A is a pre-exponential factor usually taken to be 120 amps/cm^{2}K^2 and $\varphi_{eV} \approx 4.7$ eV for carbon.[7] The

American Institute of Aeronautics and Astronautics

computed heat losses for r = 30 nm are ≈8 x 10⁻⁹ W/ particle at 3000 K and ≈8 x 10⁻⁶ W/particle at 4500 K. These values are considerably smaller than the sum of the conductive and evaporative terms, and make only a minor contribution to the overall energy balance. However, if the work function for soot were somewhat smaller, e.g., <4.5 eV, this term would be more competitive with vaporization.

The total heat loss for selected particle radii is plotted in Figure 2 as a function of particle temperature. The curves show a characteristic change in slope at ≈3500 K as the dominant cooling mechanism changes from conduction (T < 3500 K) to vaporization (T > 3500 K). These heat losses can then be balanced with the heat absorption term to determine the maximum temperature (for each particle size) which can be reached with a given laser intensity. This is shown in Figure 3. From this figure, we can see that a laser intensity of
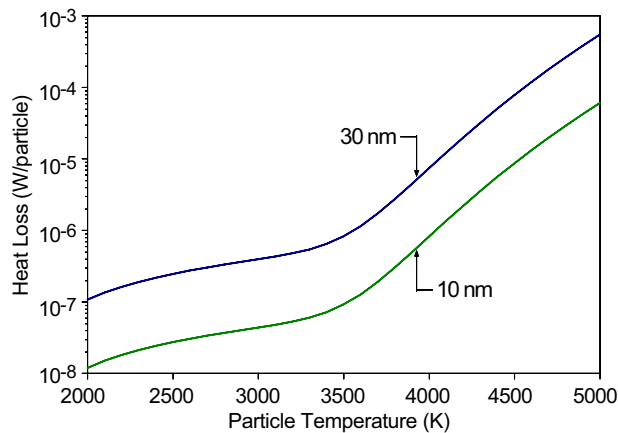
Figure 2 Total heat loss per particle (conduction+vaporization+radiation).
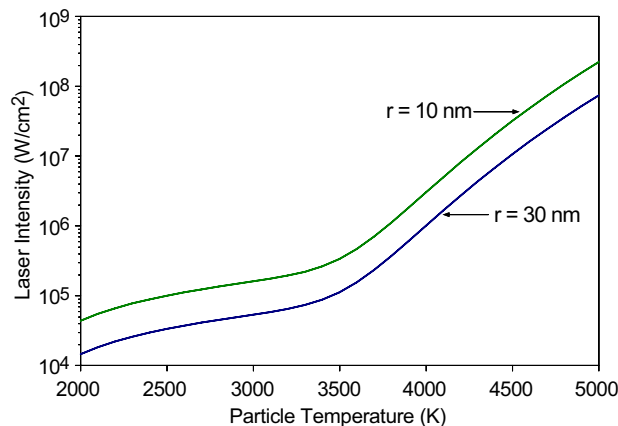
Figure 3 Critical laser intensity: intensity to balance heat input and loss.

10 MW/cm² is predicted to give a maximum temperature of 4500 K for r = 30 nm; this is the temperature above which the predictions indicate significant mass loss due to vaporization should occur. Thus the model prediction of the vaporization "threshold" intensity is consistent with our previous experimental observations.[1]

As previously shown by Melton,[2] the time-dependent LII intensity for a given laser intensity and wavelength, emission wavelength, and spectral resolution is given by

$$I(t) = \int_0^\infty N(r)\, R(r,t)\, dr$$

where N(r) is the particle size distribution as a function of the radius r, and I(t) and R(r,t) are the LII intensity and radiative response function. The response function R(r,t) describes the temporal decay in spectral radiance of a particle of radius r, which is essentially taken from numerical integration of the model equations given above.

This equation is a straightforward integral transform equation, where N(r) is transformed by the kernel function R(r,t) to give the observable I(t). If R(r,t) is well described by the heat transfer/vaporization model, it should be possible to invert the measured I(t) data to determine the size distribution N(r). This is straight-forward if a parametric functional form for N(r) can be assumed, e.g. the log-normal distribution commonly assumed for nucleating soot particles in laboratory atmospheric flames. However, the power of the tech-nique for practical systems is greatly enhanced if a generalized solution can be determined for N(r) inde-pendently of expectations for its functional form. The I(t) equation is a generalized Fourier transform equation, specifically a Fredholm equation of the first kind, and its inversion to solve for N(r) can be performed numerically using minimization methods as discussed by Press et al.[8]

As suggested by the model described above, the ability to make accurate determinations of soot volume fraction and particle size using LII will be dependent on certain experimental parameters. The characteristics of both the pump laser and the detectors used to monitor the emission must be well known. For example, it is apparent that excessive laser intensity may create a perturbation to the particle size distribution through

evaporative mass loss and thus lead to errors. In addition, to resolve and interrogate the nanosecond-scale heating and cooling trends in the vicinity of the laser pulse, fast detector response is necessary. In the following section we will describe measurements aimed at determining the effects of varying laser intensity on the short timescale LII signal characteristics. Then, results from particle sizing experiments which focus on particle cooling after the laser pulse will be shown.

Experimental Results and Discussion

Effects of Laser Intensity

Measurements have been performed in a laminar diffusion flame to determine the effects of laser intensity on the LII signal characteristics during the laser heating pulse. The diffusion flame facility has been designed to replicate flames which have been extensively studied by others to allow direct data comparison.[3] Figure 4 shows a diagram of the experimental setup. An ethylene-air diffusion flame is stabilized at the exit of a 11.1 mm diameter tube flowing pure fuel. An annular co-flow over-ventilates the flame and reduces shear and buoyancy driven instabilities providing a stable conical flame. The flows are confined using a 10.2 cm diameter quartz chimney with flat windows bonded on the sides for optical access. The fuel and air flowrates are held fixed at 3.85 and 1000 cm^3/s, respectively. The visible flame height is 88 mm.
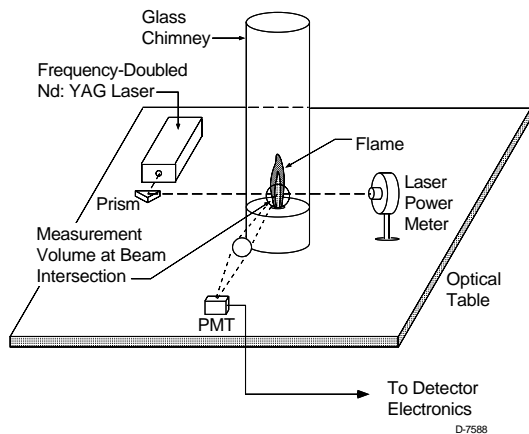

Figure 4 Schematic diagram of experimental configuration.

To heat the soot particles in these experiments, the second harmonic (λ=532 nm) of a pulsed Nd:YAG laser (Big Sky CFR 200) was used. The laser energy was varied using a calcite polarizing beamsplitter where the transmitted pulse energy could be continuously varied

between approximately 3 and 130 mJ without affecting the pulse temporal profile. To minimize measurement errors due to composition gradients in the diffusion flame, high spatial resolution was necessary. To accomplish this, the laser beam was passed through a slit aperture (not shown in Figure 4), which produced a 0.86 mm wide by 3.6 mm high beam in the probe volume. The length of each laser pulse was 10.8 ns FWHM.

The LII signal was collected using a single lens with unity magnification and focused on a photomultiplier tube (PMT: Hamamatsu H5783-01). A narrow bandpass interference filter centered at 750 nm (10 nm FWHM) and a color glass filter (Corning 2-62) were placed in front of the PMT to block the Mie scattering of the laser beam. The laser was pulsed at a rate of 10 Hz, and the average LII signal from 100 shots was recorded on a digital oscilloscope. The measurement volume in the flame was defined by the width of the laser beam and a 0.7 mm diameter aperture placed in front of the PMT. The resulting volume measured 0.7 x 0.7 x 0.86 mm^3 (H x W x D).

The effects of incident laser intensity on the LII signal characteristics at short times have been investigated. It has been previously established that for fixed soot properties, the peak LII signal level rises linearly with increasing laser intensity up to a point. When the laser intensity exceeds a certain value, the LII signal becomes nearly constant. This apparent saturation has been attributed to the attainment of a particle temperature approaching the vaporization temperature of approximately 4500 K. The present measurements are intended to investigate the sensitivity of signal saturation to local soot properties in the flame. These measurements were obtained along the centerline axis of the flame at various flame heights. The soot particle size and volume fraction vary along the centerline. It has been reported that the soot volume fraction changes by more than a factor of five[3] and measurements of primary and aggregate particle diameters indicate similar variations[9-12] as one traverses the axis from z = 1.5 to 5 cm. This facilitates the investigation of the sensitivity of the LII signal to the pump laser intensity as a function of local soot properties. Figure 5 shows the normalized LII signal as a function of incident laser intensity for three different heights in the flame. These LII data were acquired by measuring the PMT signal
level 30 ns after the tail of the laser pulse profile. The

American Institute of Aeronautics and Astronautics
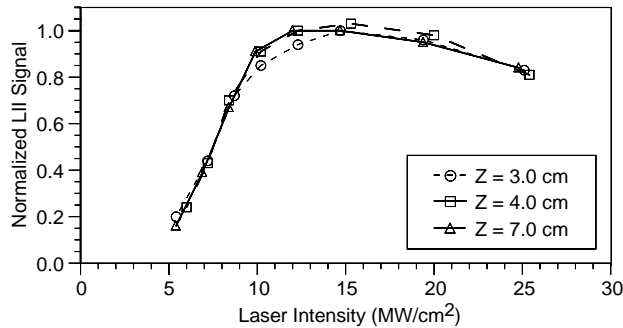
Figure 5 Normalized LII signal intensity as a function of incident laser intensity for different flame heights (750 nm detector bandpass).

data from all three axial locations yield similar curves which show saturation at approximately 12 MW/cm^2. These results suggest that the non-linear behavior, or saturation process, is only weakly sensitive to the local soot properties .

Figure 6 shows temporally resolved profiles of the PMT signal during the first 85 ns of six seperate LII measurements. All measurements were performed at an axial location of 5.0 cm on the burner centerline. Each curve in Figure 6 was obtained with a different incident laser intensity. The solid curve shows the laser pulse profile. The data indicate that for laser intensities less than approximately 12 MW/cm^2 the LII signal is con-tinually rising over the entire duration of the laser pulse and reaches a maximum value near the tail of the pulse. However, for laser intensities greater than ~12 MW/ cm^2 the LII signal reaches a maximum before the end of the laser pulse and then decays. The rate of this decay increases with laser intensity. These data suggest that for high laser intensities, the soot properties are somehow modified during the laser heating event which results in a signal decrease before the end of the pulse.
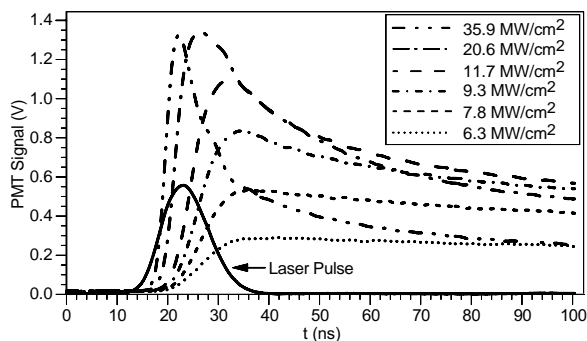
Figure 6 Temporally resolved signal profiles for various incident laser intensities (750 nm detector bandpass).
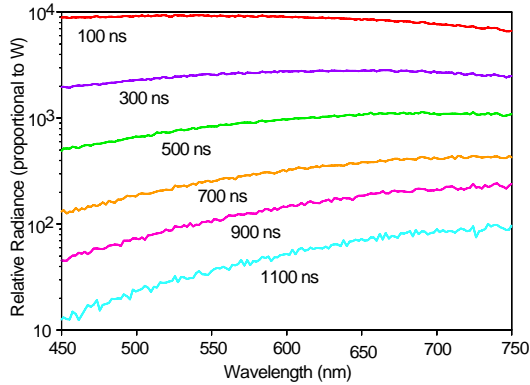
Particle Sizing Experiments

Particle sizing measurements have been performed in a flat flame burner. A description of this burner has been given previously[1] and will not be repeated here. The flat flame apparatus produces a premixed flame which has a nearly uniform temperature and composition in the cross-stream direction. The measurements presented below were performed in a premixed ethylene-air flame with the measurement volume near the centerline. The sooting tendency of the flame could be controlled by adjusting the equivalence ratio, φ.

The LII was produced using a pulsed Nd:YAG laser (Quantel Model YG580) whose output was frequency doubled. The average laser output energy was constantly monitored using a power meter. The laser pulse energy could be continuously varied between approximately 15 and 350 mJ/pulse by varying the angle of the frequency doubling crystal. For the point measurements described below, the laser output beam was unfocussed with a beam diameter of ~ 8 mm.

Time-resolved measurements of the LII spectrum were acquired using a 0.25 m monochromator (ISA Instruments, SA Inc., Model HR-320) with an intensified optical multichannel array (OMA, Princeton Instruments Inc. Model IPDA-700 G/RB) mounted at the exit. The monochromator was calibrated for relative responsivity using a NIST traceable tungsten filament lamp (Optronic Laboratories Model L-555). The OMA intensifier was gated for a 30 ns exposure time using a digital delay generator. To determine the spectral characteristics of the LII emission during particle cooling, the gate delay was varied from 0 µs to 1.1 µs while the gate width remained fixed. The gate delay was measured from the trailing edge of the laser pulse to the rising edge of the gate pulse. The spectral data presented below are multi-shot averaged data from 250 laser pulses.

The measurement volume in the flame was defined by the intersection of the projected rays from the mono-chromator input slit through the collection lens and the LII pump laser beam and measured 8 x 3.5 x 8 mm^3 (H x W x D). The experimental setup for the particle sizing measurements was similar to that shown in Figure 4 with the PMT replaced by the monochromator.

Representative response-corrected LII spectra are illustrated in Figure 7 for six different delay times. The
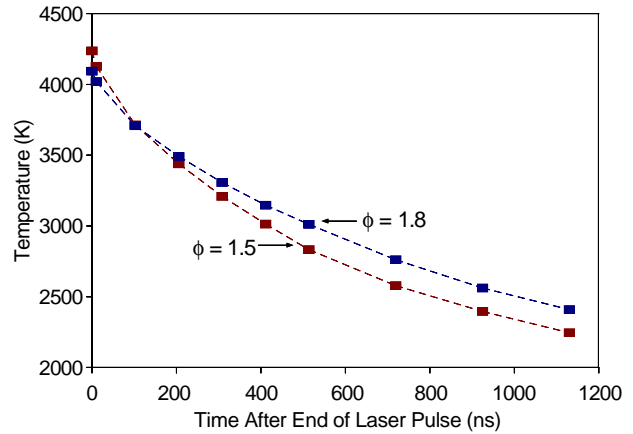
American Institute of Aeronautics and Astronautics

Figure 7 Characteristic time-resolved LII emission spectra.

Figure 8 Temperature decays from blackbody function fits of time-resolved spectral emission.

Figure 9 Comparison of theoretical and measured particle cooling rates (solid and dashed lines are model predictions).

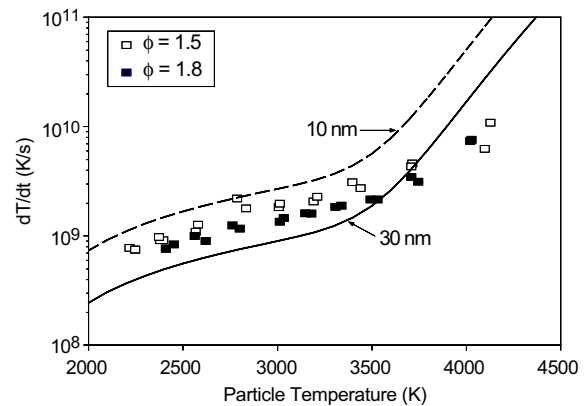measurements were taken in the flat flame (φ = 1.5) at 4 cm above the burner surface using a laser intensity of 12 MW/cm². The local soot volume fraction for these conditions was $\approx$0.8 ppm (see Ref. 1). The times in Figure 7 denote the gate delay after the trailing edge of the laser pulse profile. The emission intensities decrease rapidly with time, and the peak of the spectral distribution shifts to longer wavelengths, characteristic of particle cooling. The emissivity-corrected spectral distributions, $I(\lambda)/\sigma_a(\lambda)$, were fit to the Planck blackbody function, $N(\lambda,T)$, to determine particle temperatures.[1] It was found that the observed spectra conform well to the functional form for a single-temperature blackbody.

The soot temperatures measured in two different flames having equivalence ratios of 1.5 and 1.8 are shown as a function of time in Figure 8. The initial temperatures for the two conditions are similar in magnitude. At later times, there is a disparity in temperatures as a result of different cooling rates. The temperatures at 0 and 10 ns are likely to be under-estimated because the cooling rates at these times are too fast to be accurately observed using the 30 ns gate of the monochromator system. However, the differences in cooling at longer times can be clearly resolved. In the richer flame, larger particle sizes are expected, and slower cooling rates indicative of larger particles are measured in the φ = 1.8 flame.

The data presented in Figure 8 were used to compute the temperature decay rates shown in Figure 9. The particles were sized by comparing measured cooling rates with those predicted using the heat transfer model described above. The comparison with model predictions in the conductive cooling regime indicates

particle radii of approximately 15 and 20 nm for pre-mixed flames with equivalence ratios of ϕ = 1.5 and 1.8, respectively. Results from SEM micrographs in these flames show clusters of primary particles with mean radii of approximately 10 and 20 nm for ϕ = 1.5 and 1.8, respectively. Although the comparison between measured and calculated cooling rates is excellent in the conduction-dominated regime (T < 3500 K), at higher temperatures the cooling rates fall short of those pre-dicted by the model. This discrepancy in the vaporization-dominated regime may be explained when considering the relatively poor temporal resolution of the detector.

Conclusion

The results presented above concerning the effect of incident laser intensity on the soot particle thermal

emission temporal profile indicate that increases in laser intensity beyond 12 MW/cm^2 result in a saturation of the peak LII signal level. In addition, for the highest laser intensities used the emitted LII signal begins to decay before the end of the laser pulse. This observation is consistent with a change in soot particle properties due to excessive heating. The properties that may be perturbed include the particle mass, as has been previously demonstrated in our laboratory[1], the structure of soot agglomerates, and optical properties such as the complex index of refraction.[10] Although it has been previously shown that measurements of soot volume fraction using high laser intensities are feasible[10-13], the present data bring into question the accuracy of particle sizing when using laser intensities in excess of 12 MW/cm^2.

Particle sizing measurements in the present work were performed using an incident laser intensity of 12 MW/cm^2. The particle sizes were determined by comparing measured cooling rates with those predicted with a heat transfer model. The comparison was excellent in the conductive cooling regime, and the measured particle radii were consistent with primary particle sizes obtained from SEM micrographs. The present measurements of both particle size and temperature support the notion that the LII signal characteristics are dominated by emission from the primary soot particles. The agreement between predicted and measured cooling rates in the vaporization-dominated regime may be improved by using a pyrometer having nanosecond temporal resolution.

References

1. McManus, K.R., Allen, M.G., and Rawlins, W.T." Quantitative Detection and Imaging of Soot Particles by Laser Induced Incandescence," Paper AIAA-97-0117, presented at the 35th Aerospace Sciences Meeting and Exhibit, Reno, 1997.
2. Melton, L.A., "Soot Diagnostics Based on Laser Heating," *Appl. Opt.* 23, 2201 (1984).
3. R.J Santoro, H.G. Semerjian, and R.A. Dobbins, *Combust. Flame 51*, 203 (1983).
4. S.A. Schaaf and P.L. Chambre, "Flow of Rarified Gases," Section H of Fundamentals of Gas Dynamics, H.W. Emmons, Ed., Princeton University Press, Princeton, NJ, 1958.
5. G.E. Caledonia, N.H. Kemp, and G.A. Simons, "Endo Optical Masking Study," PSI-TR-125, Physical Sciences Inc., Final Report to Space and Missile Systems Organization, SAMSO-TR-78-95, July 1978.
6. E.Y. Lo, W.T. Laughlin, A.H. Gelb, and L.G. Piper, "Laser Ablation Process: Plume Physics," PSI-1229/TR-1422, Physical Sciences Inc., November 1995.
7. D.R. Dudek, D.A. Wright, J.P. Longwell, A.F. Sarofim, and J. Yeheskel, "Charge Loss from Heated Particles Levitated in an Electrodynamic Balance," *Combust. Sci. and Tech.* 73, 447 (1990).
8. W.H. Press, S.A. Teukolsky, W.T. Vetterling, and B.P. Flannery, Numerical Recipes, Second Edition, Cambridge University Press, 1992, p. 779 ff.
9. Dobbins, R.A., Fletcher, R.A. and Lu, W.,"Laser Microprobe Analysis of Soot Precursor Particles and Carbonaceous Soot," *Combust. Flame* 100,301 (1995).
10. Vander Wal, R.L.,"Laser-induced incandescence: detection issues," *Applied Optics* 35,6548 (1996).
11. Dobbins, R.A., Santoro, R.J. and Semerjian, H.G.,"Analysis of light scattering from soot using optical cross sections for aggregates," *Tewnty-Third Symposium (International) on Combustion*, p. 1525 (1990).
12. Puri, R., Richardson, T.F., Santoro, R.J. and Dobbins, R.A.,"Aerosol Dynamic Processes of Soot Aggregates in a Laminar Ethene Diffusion Flame," *Combust. Flame* 92,320 (1993).
13. Vander Wal, R.L.,Choi, M.Y. and Lee K.O.," The Effects of Rapid Heating of Soot: Implications When Using Laser-Induced Incandescence for Soot Diagnostics," Combust. Flame 102, 200 (1995).
14. Quay, B., Lee, T.W., Ni, T. and Santoro, R.J., "Spatially Resolved Measurements of Soot Volume Fraction Using Laser-Induced Incandescence," Combust. Flame 97, 384 (1994).
15. Wainner, R. and Seitzman, J.M.,"Soot Analysis in Combustion Environments by Laser-Induced Incandescence," Paper AIAA-97-2382, presented at the 28th Plasmadynamics and Lasers Conference, Atlanta, 1997.
16. Wainner, R. and Seitzman, J.M.,"Simultaneous Measurement of Soot Properties by Laser-Induced Incandescence," Paper AIAA-97-0605, presented at the 35th Aerospace Sciences Meeting, Reno, 1997.